RELIABILITY ASSESSMENT OF SOLDER JOINT USING BGA PACKAGE – MEGTRON 6 VERSUS FR4 PRINTED CIRCUIT BOARDS

by

MUGDHA ANISH CHAUDHARI

Presented to the Faculty of the Graduate School of
The University of Texas at Arlington in Partial Fulfillment
of the Requirements
for the Degree of

MASTER OF SCIENCE IN MECHANICAL ENGINEERING

THE UNIVERSITY OF TEXAS AT ARLINGTON

May 2017

Acknowledgements

I would like to thank Prof. Dereje Agonafer for his continuous support and guidance in my master's study and research. I would also like to thank him for his patience, motivation and enthusiasm in this project. A special thanks to him for letting me be a part of his EMNSPC team. I would also like to thank Dr. A.Haji-Sheikh and Dr. Fahad Mirza for being a part of my thesis committee.

I would like to thank my entire EMNSPC team member. A special thanks to Unique Rahangdale, Pavan Rajmane, Aniruddha Doiphode, Rishikesh Tendulkar, Navya Kesireddy and Manjarik Mrinal for their continuous guidance and motivation. Special thanks to Sally Thompson and Debi Barton for assisting me through my degree program.

A special thanks to my family and friends for their continuous support, care and motivation. Thank you all for always being there.

April 17, 2017

Abstract

RELIABILITY ASSESSMENT OF SOLDER JOINT USING BGA PACKAGE – MEGTRON 6 VERSUS FR4 PRINTED CIRCUIT BOARDS

MUGDHA ANISH CHAUDHARI, MS

The University of Texas at Arlington, 2017

Supervising Professor: Dereje Agonafer

When it comes to the mechanical and electrical seam of the Printed Circuit Board (PCB) and package, reliability of the board plays a major impact on PCB. As the frequency increases, losses in signals increase. This necessitates the use of new materials for such applications. Nelco 4000-13EPSI, Rogers 4350B, Panasonic Megtron 6 are few high-speed materials used. Studies have shown that Megtron 6 has the least dielectric losses so far, low transmission loss, high heat resistance and has low weight loss than the FR-4 boards. With an increasing demand for high performance, reliability and lower costs, the field of electronic packaging has a vast area to research on. Ball Grid Array (BGA), a type of Surface Mount Technology package has and continues to be used due to its robust design, improved performance, reduced package thickness and large number of pins on an efficient board area. As such, in this paper, we study reliability of BGA package on various boards.

In this work, we use Megtron 6 and FR4 circuit boards with BGA packages. A Dynamic Mechanical Analyzer (DMA) is used to obtain the time and temperature dependent viscoelastic properties of the boards while the Coefficient of Thermal Expansion (CTE) and glass transition temperatures are obtained from the Thermo-Mechanical Analyzer (TMA). The results obtained from characterization of both the boards are used to simulate Finite Element Analysis (FEA) model. ANSYS Workbench 18 is leveraged to study the life to failure of the package and its effect on the solder ball reliability using both the boards under different thermal loadings. We also compare the plastic work for these boards which play a significant role in the reliability of a package assembly.

Table of Contents

List of Illustrations

List of Tables

Chapter 1

INTRODUCTION

1.1 Electronic Packages

Electronic packages are used to protect integrated circuits from mechanical, thermal, electrical and chemical damage. According to the Moore's law, Integrated circuits are getting smaller and complex day by day which makes it difficult to protect them. The numbers of interconnections are increasing with the increase in transistor density coming from the chip to the substrate. Electronic packaging and materials used for printed circuit boards (PCB) and packages have to evolve with increasing use of high frequency high speed devices with enhanced capabilities.

1.2 High frequency laminates

High frequency laminates provide better and improved electrical performance. Improved impedance control, low moisture absorption, good thermal management are few advantages of high frequency laminates. . The literature shows a more consistent performance in thermally dynamic environment [3]. High frequency laminates show much better performance than FR4. Reliability, fabrication, performance, material properties are few issues that can be faced while using high frequency laminates. High speed, high frequency laminates like Nelco N4000-13, Isola FR408, and Panasonic Megtron 6 have low dielectric constant (Dk) and low loss tangent [9].

1.3 Moore's Law

Moore's law was predicted by Gordon E. Moore, Co-founder of Intel where he predicted the pace of silicon technology. This law was accepted and followed by many companies and is still followed by many. This law stated that" The overall processing power for computers will double every two years" which means that the number of transistors in a CPU would double in every two years. The following image shows a graph for Moore's law.

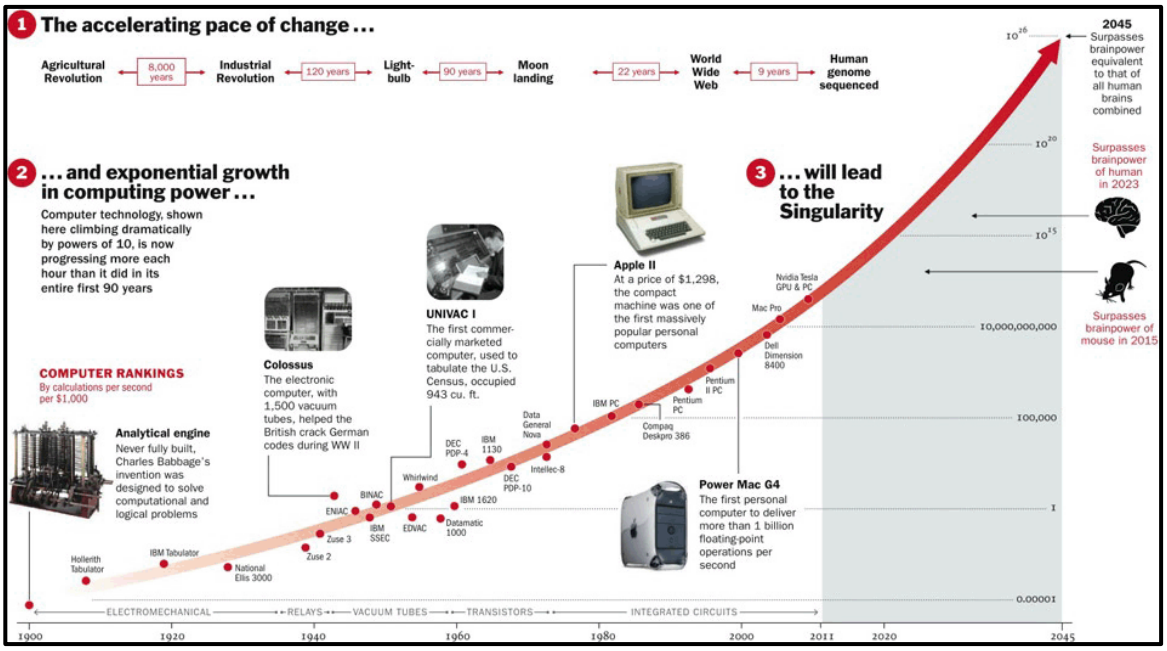

Figure 1.1: Moore's Law Graph

1.7 Integrated Circuits

Integrated circuits are also known as monolithic integrated circuit which comprises of a set of electronic circuit on one small flat chip or plate of semiconductor material (Silicon). Integrated circuits are usually everywhere as an oscillator, microprocessor, amplifier and many more. With decreasing size of computer, cell phones, electronics the size of the chips or integrated circuits are also reducing. The cost for integrated circuits is reducing too.

There are different types of integrated circuit packages depending on how they are mounted such as surface mount integrated circuit package, through hole mount integrated circuit package and contactless mount integrated circuit package. The following figure shows a tree chart of different types of integrated circuit packaging techniques used.

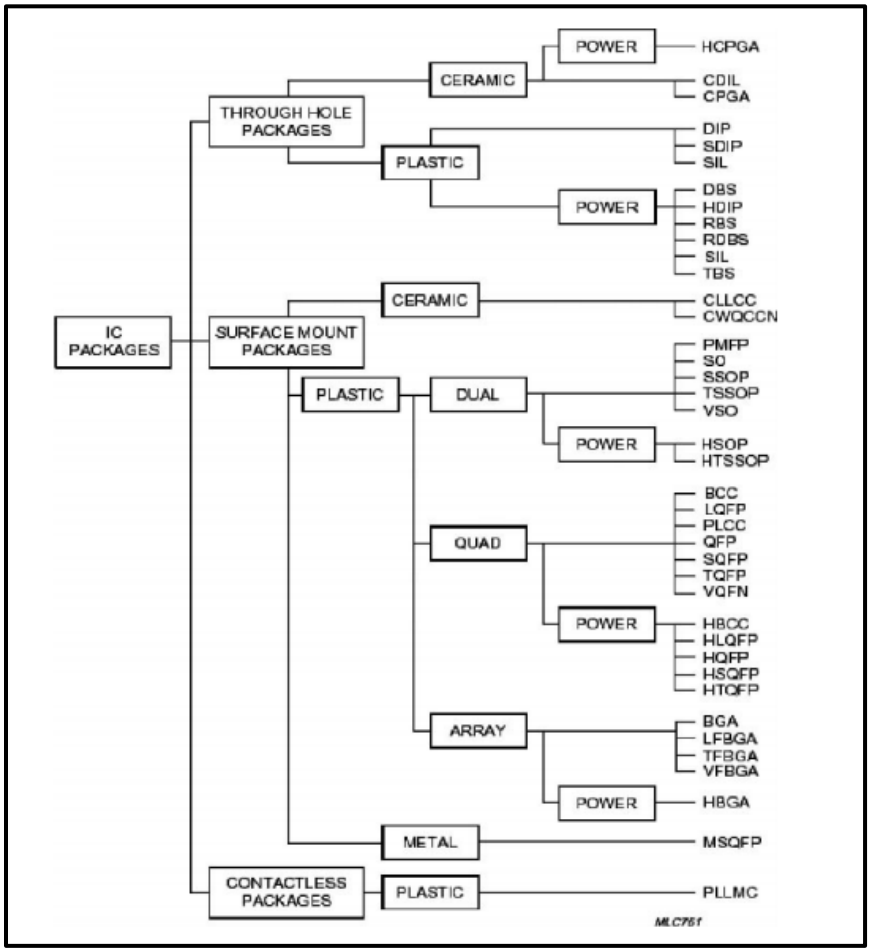

Figure 1.2: Different Types of IC Packaging Techniques

1.5 Ball Grid Array (BGA) Package

BGA is a surface mount technology package used to permanently mount devices such as microprocessors. This package provides more interconnection pins that can be put on a dual in-line or flat package. Complete bottom surface of BGA package is available for interconnections. BGA package has shorter leads and better performance at high speed. This package with a large number of interconnects have a robust design. The underside of this package is used for connections instead of the perimeter unlike the QFN package. In a BGA package the solder balls or bumps are placed in a grid, hence the

name Ball Grid Array package, for connectivity on the bottom side of the package or carrier chip BGA has lower thermal resistance as compared to that of the QFN package.

Types of BGA package are as follows:

MAPBGA – Molded Array Process Ball Grid Array

PBGA – Plastic Ball Grid Array

TEPBGA – Thermally Enhanced Plastic Ball Grid Array

TBGA – Tape Ball Grid Array

MicroBGA

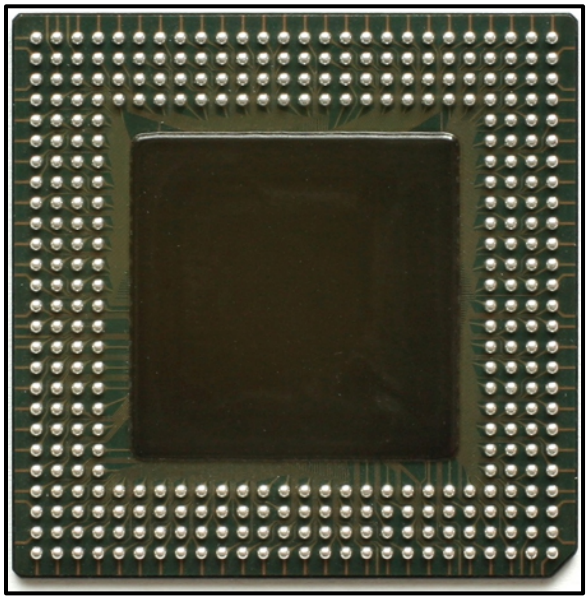

Figure 1.3: Ball Grid Array Package

1.6 Motivation and Objective

We have a lot of literature on high frequency laminates comparing its properties to other materials like the dissipation factor, moisture absorption factor, dielectric constants but nothing much on the reliability of these laminates. In this work we compare the solder ball reliability of Megtron 6 and FR4 boards using BGA package. BGA is an extensively used Surface Mount Technology package. Development in BGA and its robust design encourage us to use this package for our study. We study the effect of Accelerated Thermal Cycling (ATC) on the solder joint for a BGA package using ANSYS Workbench18. After performing ATC, the plastic work of the two boards is compared. ATC is applied from -40^0C to 125^0C with a dwell and ramp time of 15 minutes. We also compare equivalent stresses, equivalent strains, directional deformations and life to failure using Syed's Model [14]. Similarly, we compare the performance of Megtron GX, Megtron 4s, Megtron 4, Megtron 7 and Megtron 2.

Chapter 2

LITERATURE REVIEW

John Coonrod [3], has discussed about the use of FR4 and high frequency laminates. The author has basically compared basic material properties, circuit fabrication issues, reliability issues, general end-use consideration, electrical performance consideration and hybrid multilayer PCB for FR4 and high frequency materials. In this article the author has provided few guidelines to understand when to use a high frequency material and when to use FR4. A discussion on hybrid boards is also done where a combination of FR4 and high frequency laminate is used.

Unique Rahangdale [1] in his paper has done a comparative study of RCC and FR4 BOARDS. The reliability of these boards was characterized in this paper using different machines and results were used for finite element analysis. Directional deformation, equivalent stresses and strains, change in plastic work was obtained from computational analysis using ANSYS. In this paper, advantages of both RCC and FR4 boards were stated. Depending on the demand the two boards can be used as stated in this paper.

Sanjay Mahesan Revathy [4] in this thesis work he has varied the thickness of copper layers and stiffness of prepreg layers. A comparative study was done to predict the life to failure of the BGA package. In this work the main cause behind the solder joint failure was analyzed and a reliable design was obtained.

Chapter 3

MATERIAL CHARACTERIZATION

It is crucial to acquire accurate material properties of a board for Finite Element Analysis. Coefficient of Thermal Expansion (CTE), Young's Modulus, Storage Modulus (E') and Loss Modulus (E") are obtained through material characterization. We use the Thermo Mechanical Analyzer (TMA) to obtain the CTE value while Young's Modulus, Storage Modulus and Loss Modulus are obtained using Dynamic Mechanical Analyzer (DMA)

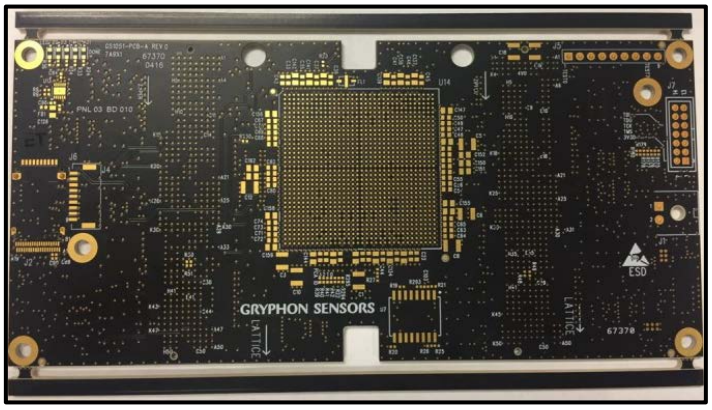

Figure 3.1: Front view of Megtron 6 board used in this study

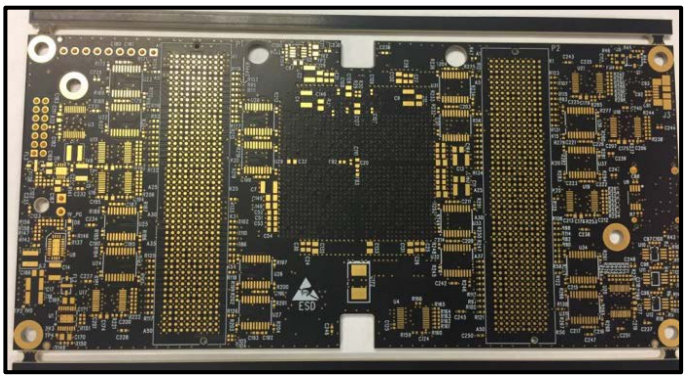

Figure 3.2: Back view of Megtron 6 board used in this study

3.1 THERMAL MECHANICAL ANALYZER (TMA)

3.1.1 Coefficient of Thermal Expansion (CTE):

The rate by which a PCB material expands due to heat is called the Coefficient of Thermal Expansion (CTE).CTE can also be defined as the fractional change in length per degree of temperature change

$$\alpha = \frac{\epsilon}{\Delta T}$$

Where,

α – Coefficient of Thermal Expansion (CTE)

$\boldsymbol{\epsilon}$- Strain (mm/mm)

ΔT - Difference in Temperature (^{0}C)

3.1.2 Glass Transition Temperature (Tg):

At this temperature range the polymer chains become more mobile and the PCB substrate transitions from a glassy rigid state to a softened deformable state. The properties are regained once the material cools back to room temperature.

3.1.3 Decomposition Temperature (Td):

At this temperature the PCB material chemically decomposes and it can never regain its original properties upon cooling. It is said that the material losses up to 5% of its mass.

Figure 3.3: Thermo Mechanical Analyzer (TMA)

TMA consists of a thermal chamber with a good working range of temperature. In-planer and out of plane CTE can be measured used TMA. A TMA sample of 8x8 mm is cut using a High Speed Cutter. The dimensions of the sample are such that it fits correctly under the probe. The Quartz probe of the TMA sets on the sample and the CTE is obtained from the relative movement of the probe. We calculate CTE from -65^{0}C to 260^{0}C with an increment of 5^{0}C /min.

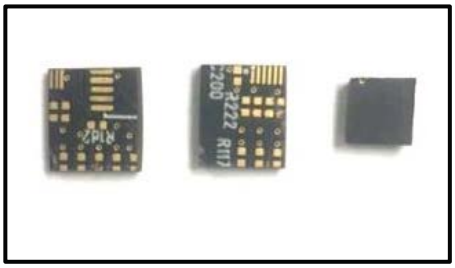

Figure 3.4: Samples used for TMA experiment

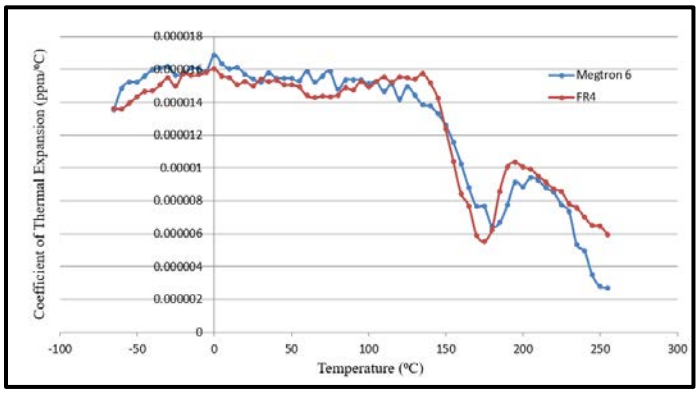

Figure 3.5: Plot for in-plane CTE

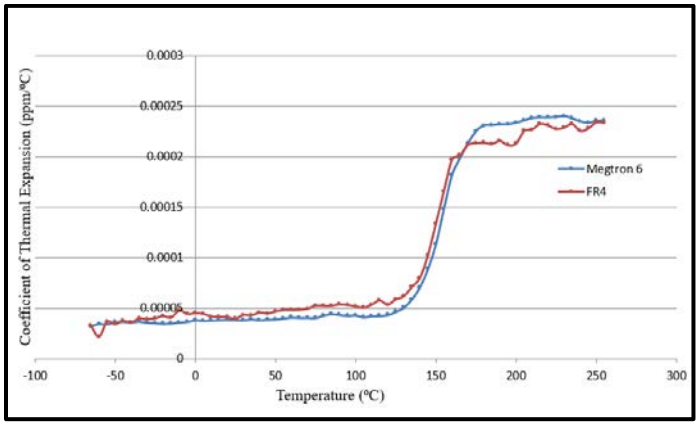

Figure 3.6: Plot for out of plane CTE

The in-plane and out of plane CTE are measured using TMA. Figure 3.5 shows plot for in-plane CTE while figure 3.6 shows plot for out of plane CTE. These coefficients of thermal expansion can be measured by keeping the board sample in three different positions under the quartz probe. A wide variety of thermal loads can be calculated by using a temperature range from -65^{0}C to 260^{0}C. A significant dip can be observed in the in-plane CTE plot after 150^{0}C. This is due to recrystallization and cold crystallization processes occurring in the sample during experiments. Further expansion of sample can be

observed above 180^0C which at the end melts. The melting process can be seen after about 225^0C with decrease in the sample height and viscosity.

Table 3.1 shows the package material properties used in this work. Poisson's ratio for the Megtron 6 board is 0.2 while that for FR4 is 0.39 [11]. Table 3.2 shows all the required material properties used in this study.

Material	CTE (ppm/^{0}C)	E (GPa)
Copper Pad	17.78	110
Die Attach	65	154
Die	2.94	150
Mold	8.43	24
Polyimide Layer	35	3.3
Solder Mask	30	4.6

Table 3.1: Material properties for a BGA package

Boards	CTE (ppm/^{0}C)			E(GPa)
	X direction	Y direction	Z direction	
FR4	15.3	13.1	41.1	15.46
Megtron 6	15.39	13.2	43.1	13.8

Table 3.2: Material Properties of Megtron 6 and FR4 boards

3.2 DYNAMIC MECHANICAL ANALYZER (DMA)

Figure 3.7: Dynamic Mechanical Analyzer (DMA)

3.2.1 Young's Modulus (E): Young's Modulus is also known as Tensile Modulus or Modulus of Elasticity. It basically measures the stiffness of a PCB. Young's Modulus can be defined as the ration of stress to strain in a particular direction. Materials that deform less as compared to other under tensile loading are said to be stiffer.

3.2.2 Storage Modulus (E'): Storage Modulus measures the stored energy representing elastic portion of a material.

3.2.3 Loss Modulus (E''): Loss Modulus measures the energy dissipated as heat, representing the viscous portion of the material.

Dynamic mechanical analyzer (DMA) or Dynamic Mechanical Thermal Analyzer (DMTA) is a testing machine which helps us to obtain stress, temperature, frequency and many other properties. A small deformation in cyclic manner is applied to the DMA sample. A sinusoidal deformation is applied to the sample. The sample is 10mm x 50mm in width and length respectively. A control stress or strain can be applied on the sample using DMA. The sample will be then deformed by a sinusoidal deformation for a given stress. The stiffness of the sample will affect the amount of deformation. A sinusoidal wave generated by a force motor is transferred to the sample through a drive shaft. The DMA sample should be placed in such a way that while conducting the experiment it should not move from its place. Figure 8 shows a DMA machine used in this paper.

Figure 3.8: Sample for DMA experiment

In this work, we also compare the performance for different Megtron series like Megtron GX, Megtron 2, Megtron 4, Megtron 7, and Megtron 4s. Properties of these materials are as in table 3.3 [11].

Material	CTE (ppm/^{0}C)			Young's Modulus	Poisson's Ratio
	x	y	z		
Megtron 4	14.5	14.5	35	15.9	0.2
Megtron 4s	14	14	32	15.1	0.2
Megtron 7	16	16	42	13.5	0.2
Megtron 2	15	15	34	16.7	0.2
Megtron GX	10	10	22	29	0.2

Table 3.3: Material properties for series of Megtron

Chapter 4

COMPUTATIONAL ANALYSIS

4.1 Introduction of Finite Element Analysis (FEA)

Finite Element Modeling or Analysis is a computational approach to solve engineering and mathematical physics problems. Vibrational, Structural and thermal analysis can be done using FEA which is used by most of the companies. FEA is used to solve problems in thermal, structural, fluids, geo mechanics, electromagnetic, hydraulics, vibrations, bio medical and nuclear engineering. FEA provide us with numerous advantages. Firstly, it gives us precise geometrical constructions. Secondly, analysis can be done using various materials of a body at the same time, i.e. different materials can be assigned to one body and analysis can be done on it.

Finite element method works on the principle which divides an element into finite number of smaller elements usually with 3 to 4 nodes. Polynomial interpolation is used to find the displacement of these nodes. Equivalent system of forces at each node replaces the load or force. The governing equation is as follows,

$$[F]= [K] \{u\}$$

Where, [F] stands for force vector, [K] is Global Stiffness Matrix and {u} is the nodal displacement. The stiffness matrix depends on the material propertied like isotropic or orthotropic and the geometry of the object. The force vector depend s on the boundary conditions and the loading along with the direction of the loading applied. The nodal displacement is obtained by mathematical methods by the software.

FEA solve problems in parts and combine the solution so as to obtain result for a complete body. This solution for structural problems helps in determining the displacement at each node and stresses in each element. Preprocessing, solution, post processing are the steps that we follow during FEA. In the Preprocessing we create a geometric model, further elements and mesh is generated and materials properties are assigned. Secondly, in the Solution, boundary conditions and loads are applied at this step. Output and load step control is selected and the solution is obtained. In the post processing step the result is reviewed.

Few assumptions are made during FEA such as considering the PCB to be orthotropic, all materials are considered to be linear elastic except the solder, solder to be modelled as rate dependent viscoplastic material using Anand's viscoplastic model.

4.2 Geometry

Figure 4.1 shows detailed cross section of a BGA package used in this paper. BGA package has copper pad on top and bottom side of the solder ball. As seen in figure 4.1, a Silicon die is attached to the Polyimide layer with a solder mask in between them. Both sides of the board, the PCB and substrate have a layer of solder mask. The below figure is a detailed schematic diagram on a BGA package.

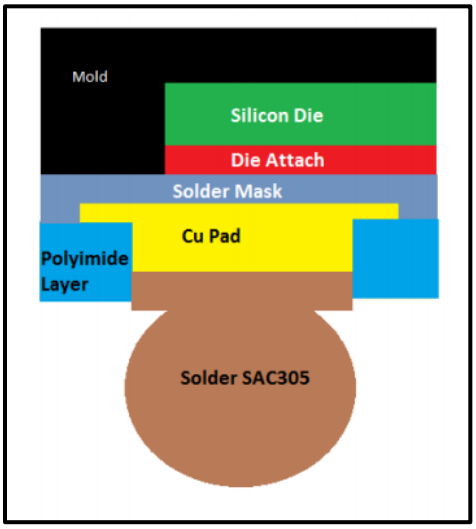

Figure 4.1: Schematic diagram for a BGA package

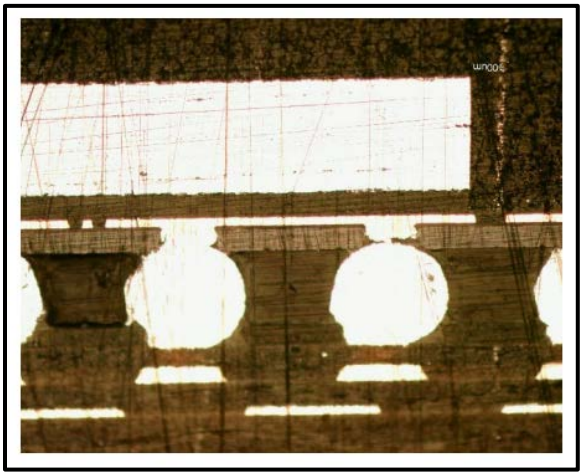

Figure 4.2: Microscopic image of a BGA package

A 3D model is developed from the X-ray image, cross sectional image of BGA and the dimensions from the drawing [2]. An octant symmetric model is used for further analysis to save the computational time as in figure 4.5. The two boards used in this paper are

Megtron 6 and FR4 where Megtron 6 consists of 18 layers (1-16-1) of copper while the FR4 board has 8 layers (1-6-1) of copper. Both the boards are approximately 2mm thick.

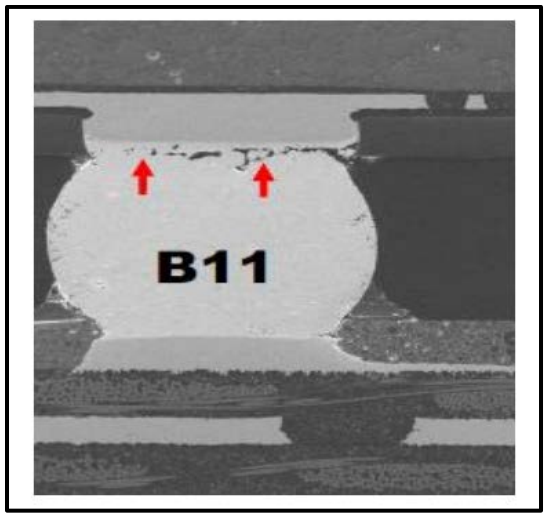

Figue 4.3: Solder ball failure towards package side

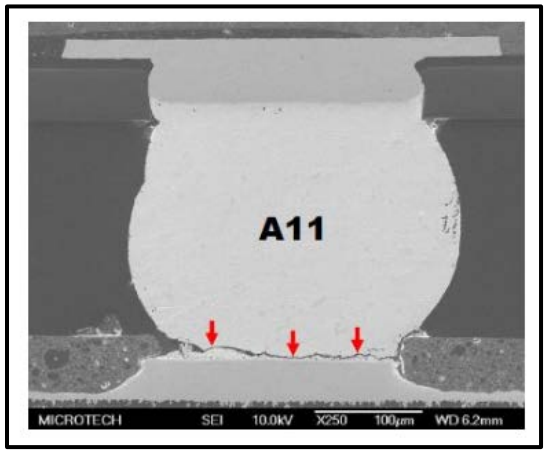

Figure 4.4: Solder ball failure towards board side

Two, 11x11 Micro star BGA package is designed with a thickness of 1mm. Solder ball reliability of this BGA package for the two boards are tested using ATC. A temperature

range of -40^{0}C to 125^{0}C with a dwell and ramp time of 15 minutes each is used for the ATC. A solder ball might fail on both the package and board side, hence it is important to perform failure analysis on these two sides. Analysis will be done depending on the results obtained in further discussions. Figure 4.3 and figure 4.4 shows failure on solder ball on the package and the board side [4].

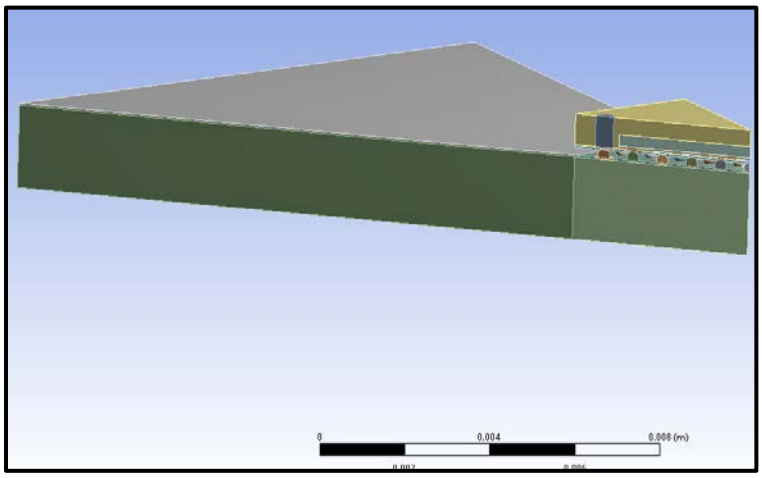

Figure 4.5: Octant symmetrical model used for the study

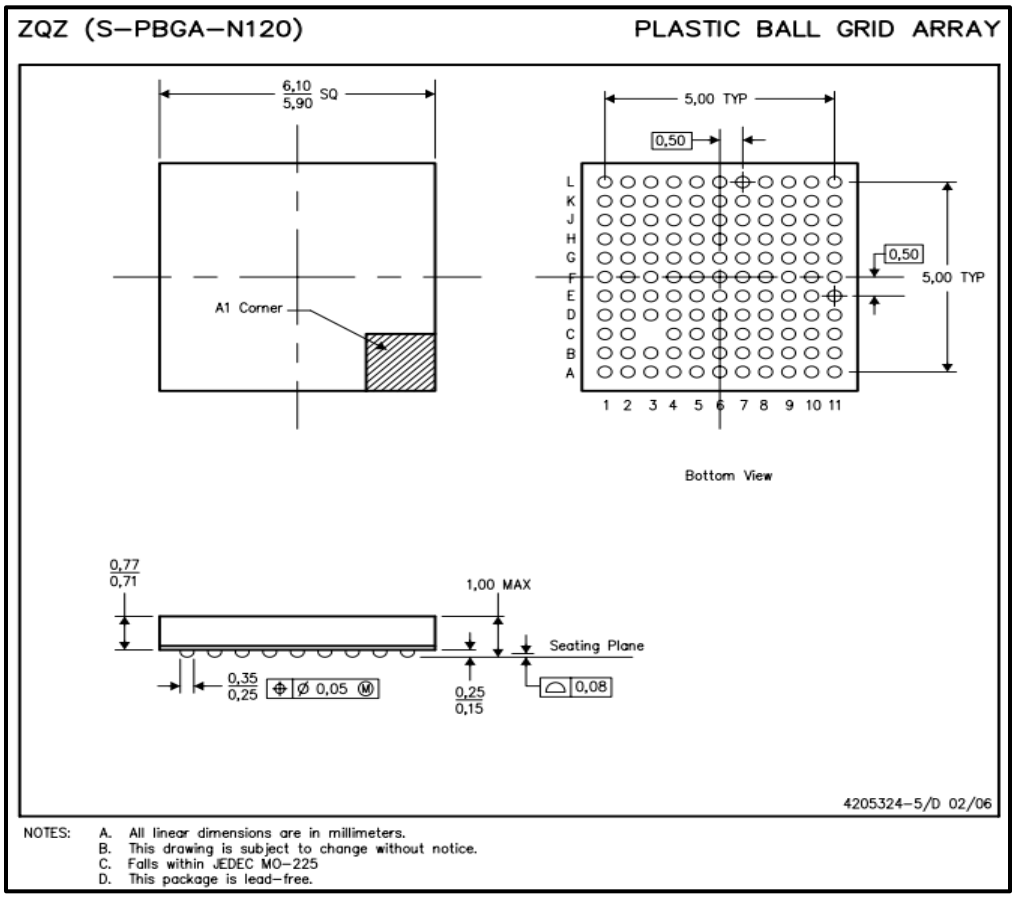

Figure 4.6: Micro star BGA drawing used to obtain unknown dimensions of BGA package

The basic configurations are obtained from the above figure 4.6.The solder ball pitch and number of solder balls is obtained from the above figures. All the dimensions are used to construct an octant symmetric model using ANSYS 18. An octant model is used so as to save the computational time.

4.3 Meshing

Hex dominant and three node elements are used in meshing this body. Critical solder ball is determined using full octant geometry by solving the solution. Figure 4.7 shows meshed octant geometry used in this work. Sub modeling is used to determine accurate results for the critical solder ball or joint. More detailed meshing is done using the sub modeling technique. Figure 4.8 shows a meshed sub model used in this work. This sub model is obtained from the octant model. [4]

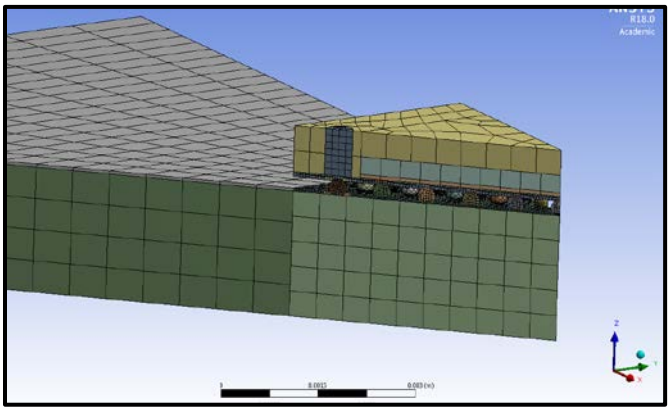

Figure 4.7: Meshed Octant symmetrical global model

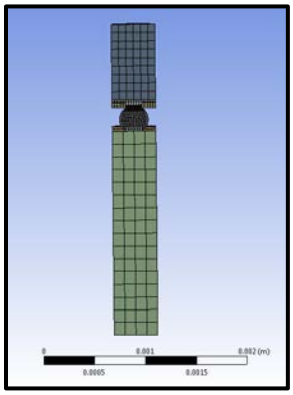

Figure 4.8: Detailed meshed sub model obtained from a global model

Displacement of the sub model is transferred using cut boundary interpolation from the global model. These are used as the boundary conditions for the local model. Accurate results are obtained using sub model due to detailed meshing.

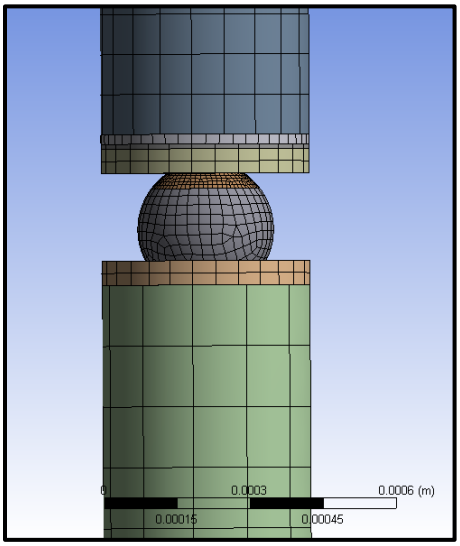

Figure 4.9: Meshed sub model

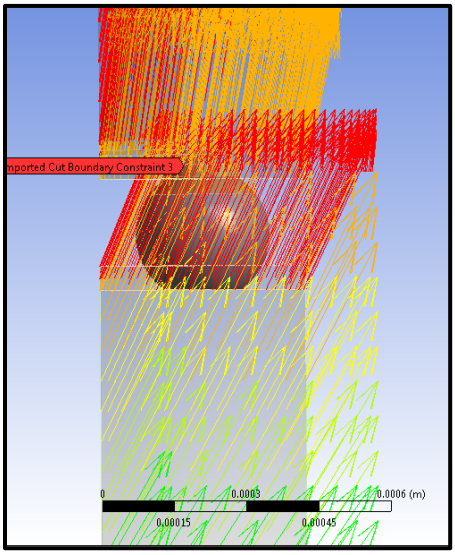

Figure 4.10: Imported cut boundary condition from global model

4.4 Material Properties and Boundary Condition

The package is considered to be linearly elastic except the solder ball and the FR4 material properties. All the material properties used in this work are as mentioned in the material characterization section. Input is given for temperature dependent CTE, temperature dependent Young's modulus, Poisson's ratio, temperature dependent shear modulus. The two inside faces where the geometry splits, are the faces where symmetric boundary conditions are applied. These two boards are considered to be linearly orthotropic in nature. Anand's model is used to elaborate the solder ball's behavior, solder ball is considered to be viscoplastic in nature. The solder ball consist of SAC 305 with 96.5% Tin (Sn), 30% Silver (Ag) ad 0.5% Copper (Cu). Using Anand's viscoplastic model, a rate dependent viscoplastic solder was modelled as per the assumptions. Both creep and plastic deformations are considered to represent secondary creep of the solder. A, Q, m, n, hu, a, su, ŝ, ξ [12]

$$\frac{d\varepsilon_{in}}{dt} = A\left[\sin h\ \left(\xi\ \frac{\sigma}{s}\right)\right]^{\frac{1}{m}} \exp\left(-\frac{Q}{RT}\right)$$

$$\dot{s} = \left\{h_0(|B|)^{\alpha}\ \frac{B}{|B|}\right\}\frac{d\varepsilon_p}{dt}$$

$$B = 1 - \frac{s}{s^*}$$

$$s^* = \hat{s}\left[\frac{1}{A}\frac{d\varepsilon_p}{dt}\exp\left(-\frac{Q}{RT}\right)\right]$$

Constant	Name	Unit	Value
s_0	Initial Deformation Resistance	MPa	12.41
Q/R	Activation Energy/ Universal Gas Constant	1/K	9400
A	Pre- exponential Factor	sec^{-1}	4E+06
ξ	Multiplier of Stress	Dimensionless	1.5
m	Strain Rate Sensitivity of Stress	Dimensionless	0.303
h_0	Hardening/Softening Constant	MPa	1378.8
$\hat{s}$	Coefficient of Deformation Resistance Saturation	MPa	0.07
n	Strain Rate Sensitivity of Saturation	Dimensionless	1.3
a	Strain Rate of Sensitivity of Hardening or Softening	Dimensionless	1.6832

Table 4.1 Anand's material constant for SAC 305

Further analysis was done using sub modelling and a detailed model was constructed [12]. The sub model is sliced from the detailed global model. A detailed picture of global model and sub model is seen from figure 4.7 and 4.8. Sub model consist of a half corner solder ball on which thermal loading is applied. Coarse meshing is done on Global modeling. Meshing is finalized after doing a mesh sensitive analysis for sub model. Cut boundary constraint is imported to sub model from the global model. A thermal loading of three cycles was applied during analysis which ranged from -40^0C to 125^0C with ramp and

dwell time of 15minutes each. A thermal cycling plot can be seen from figure 4.11. JEDEC standard JESD22-A104D is used for thermal cycling in this work.

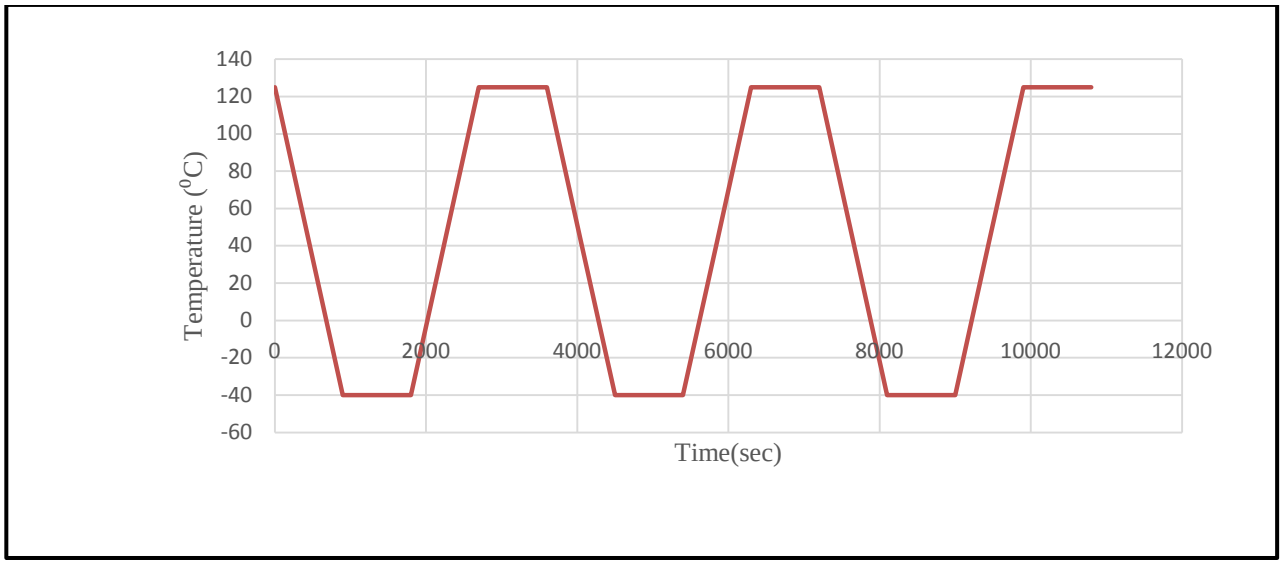

Figure 4.11: Thermal cycling plot

Chapter 5

FATIGUE LIFE PREDICTION MODEL

5.1 Introduction

The fatigue life prediction model is used to predict life cycles to failure of the package i.e. it predicts life cycle of a package which is usually between 100 to 10,000 cycles. Due to thermo mechanical failure the solder joint fails earlier giving less life to a package. Creep strain, plastic strain range and inelastic strain energy density are the fatigue damager parameters. From the board level reliability we can calculate the life to failure. Change in plastic work is used to predict the life to failure in this work. We use Syed's Model to predict the life cycles to failure which is as follows,

$$N_f=674.08\Delta W^{(-0.9229)}$$

Where, N_f is the predicted life cycles to failure and ΔW is the change in plastic work. Using the strain energy density, Syed used a SnAgCu solder material for the life prediction of CSP and BGA packages.

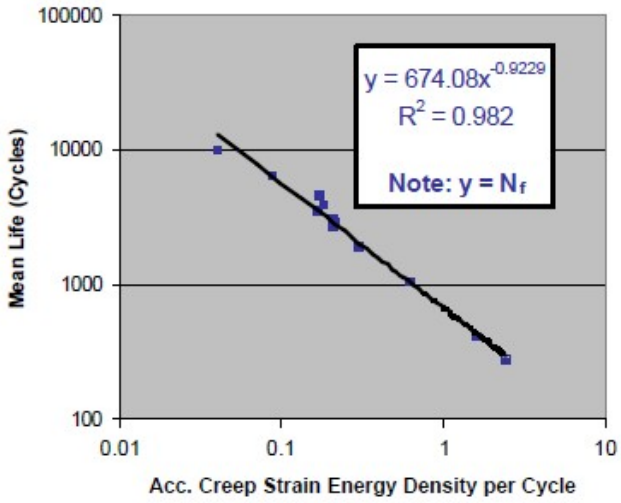

Figure 5.1: Syed's Model graph

The below figure shows a cyclic stress-strain hysteresis loop used to compare the inelastic dissipated energy that is the plastic work and the elastic strain density. This inelastic strain density is also called as the accumulated plastic work.

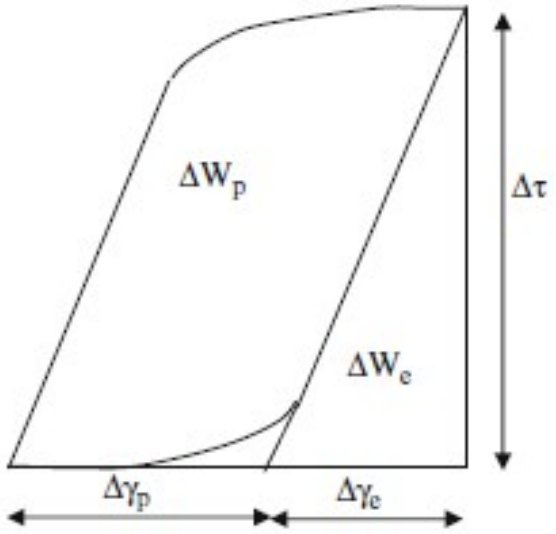

Figure 5.2: Cyclic stress-strain hysteresis loop

Chapter 6

RESULTS

A lumped model created on ANSYS 18 for computational analysis has similar meshing for Megtron and FR4 boards. Figure 4.7 shows a lumped model used for computational analysis. All the required material properties have been defined separately. Simulations for all the boards are done keeping the mesh same for all the boards.

Maximum stresses are seen on the corner solder ball towards the package side. The Equivalent stress distribution comparison for Megtron series and FR4 is as shown in figure 6.1. Maximum Von Misses stresses are developed in FR4 board than any other Megtron material. The developed stresses are least in Megtron GX while as compared to Megtron 6 and FR4, Megtron 6 shows least stress. It can be seen from the figure 6.2 that maximum stresses are developed on the corner solder ball.

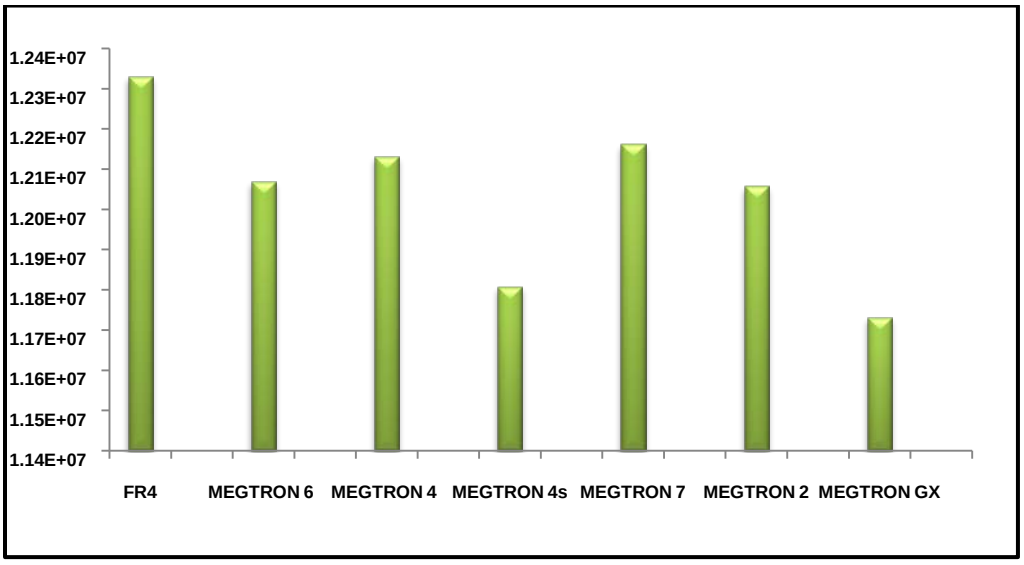

Figure 6.1: Plot for equivalent stress at corner solder ball (Pa)

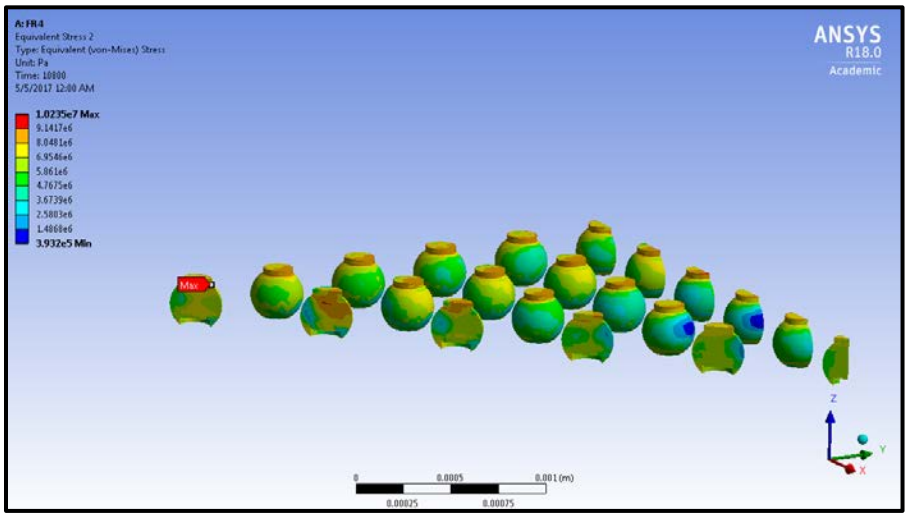

Figure 6.2: Maximum stress at corner solder ball

A similar trend is seen for the Equivalent elastic strain for these boards. The board with FR4 shows the highest strain. Strain in Megtron 6 is less than that of the FR4 board. Figure 6.4 show equivalent elastic strain graph. Equivalent stress and strain are higher in FR4 which shows that the FR4 board is stiffer than the Megtron 6 board. Maximum elastic strain is observed at the top side of the corner solder ball which can be seen from figure 6.3 [10].

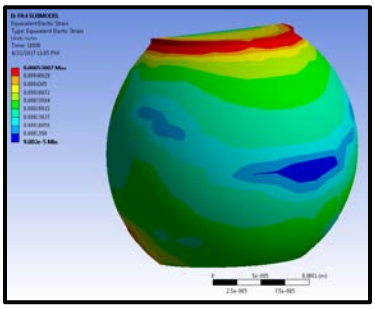

Figure 6.3: Maximum elastic strain towards the package side

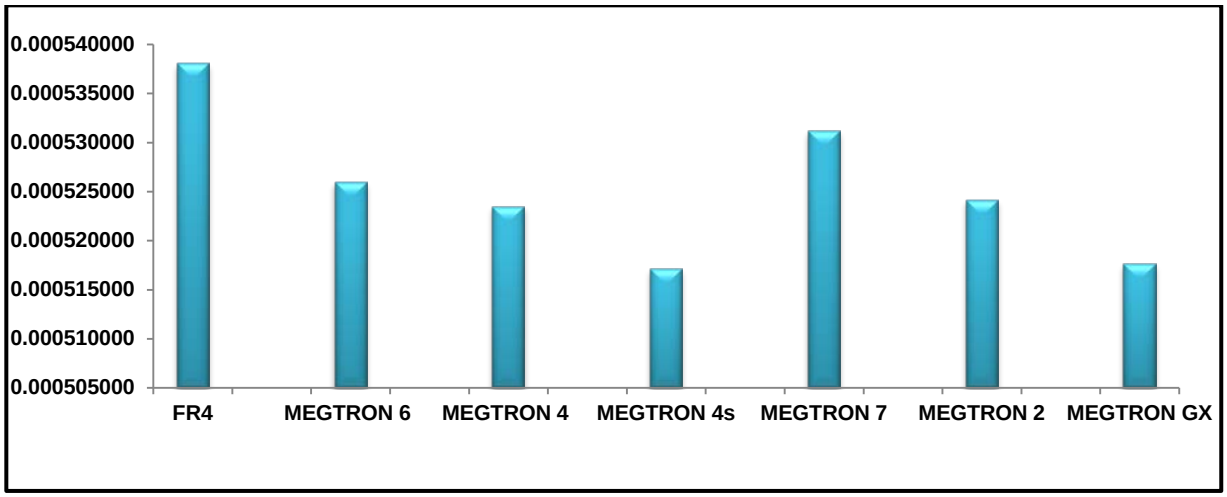

Figure 6.4: Plot for equivalent elastic strain

The directional deformation for the boards can be seen from figure 6.5 and figure 6.6. The deformation in z axis is more than that of the x and y directions. This is because fiberglass is woven in x and y directional which restricts the expansion of the material in these directions hence the material expands in the z direction. Also, deformational in Megtron 6 is less than that of the FR4 board which is because the out of plane CTE of Megtron 6 is less than that of the FR4 board.

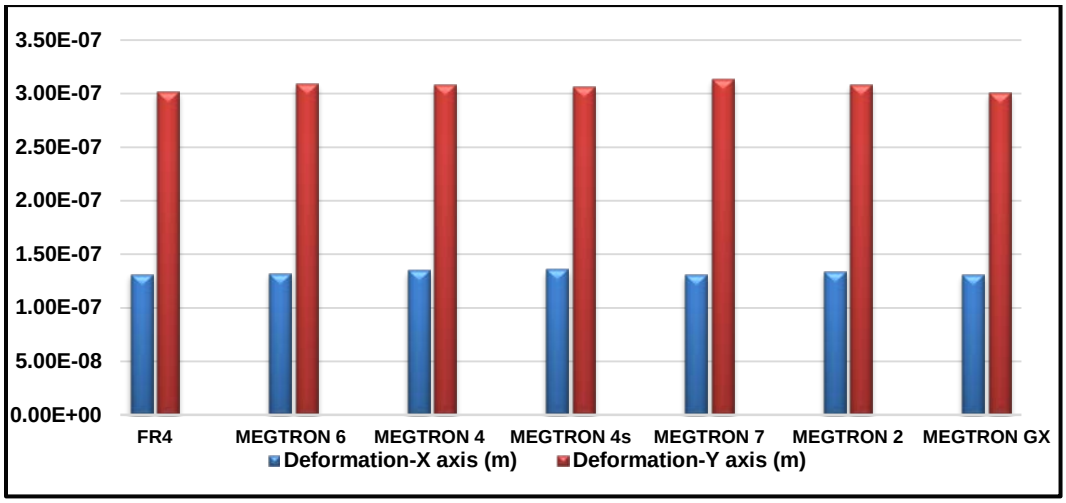

Figure 6.5: Plot for deformation in x and y directions

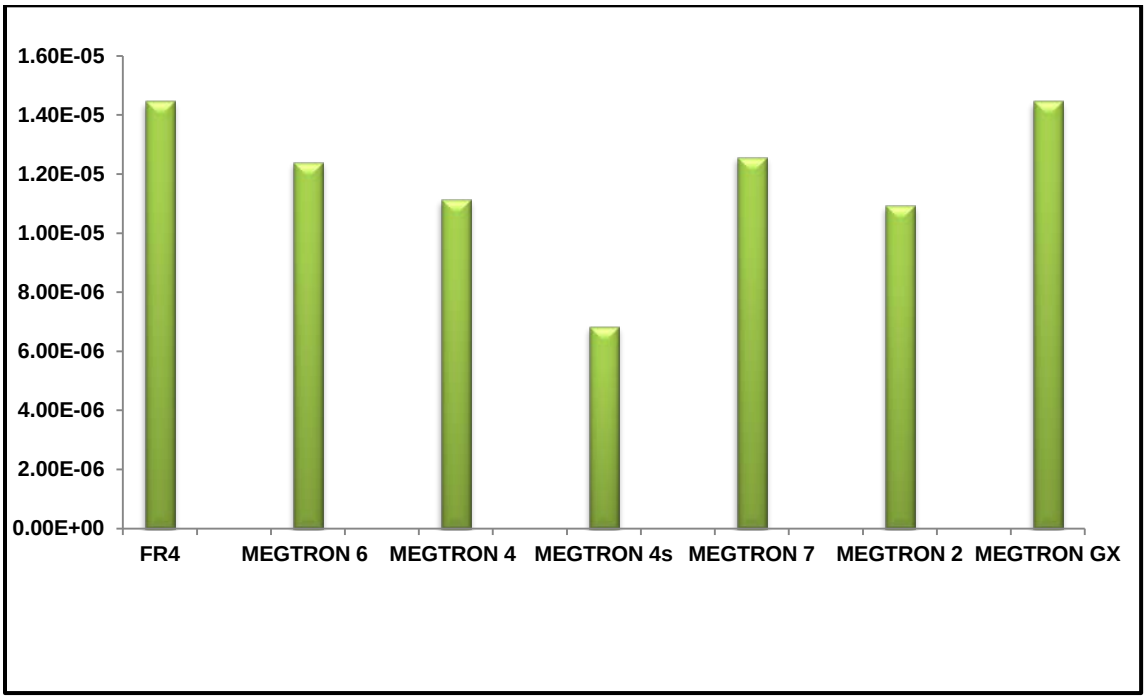

Figure 6.6: Plot for deformation in z direction

It is important to calculate the change in plastic work as the solder ball is not flexible and will continue to deform it which eventually fails by cracking. We consider both sides of the solder ball to calculate the change in plastic work of the boards as the solder ball can fail on both the directions due the mismatch in CTE on both the package and board side. The change in average plastic work is calculated between the second and third cycle using Darveaux's APDL code. Figure 6.7 shows the trend in change in plastic work for the boards. The plastic work for Megtron 6 is about 25% less than that of the FR4 board. While Megtron 4s shows the least change in plastic work.

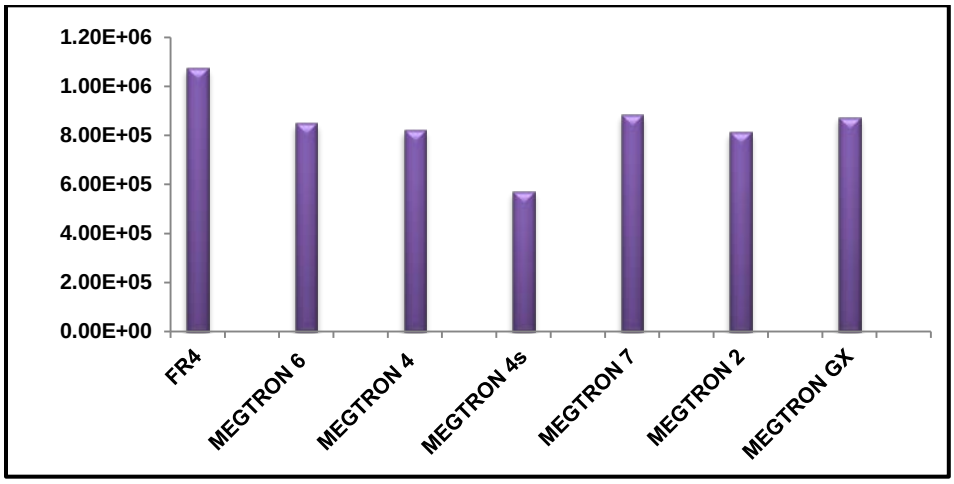

Figure 6.7: Plot for change in plastic work

Life to failure is calculated using Syed's Model, [14]

$$Nf = 674.08\Delta W\ (-0.9229)$$

Where Nf is Predicted life cycles to failure and ΔW is change in plastic work. From the calculations, it was seen that the Megtron 6 board is 24% more durable than the FR4 board. Figure 6.8 shows a graph for Life to failure using Syed's Model.

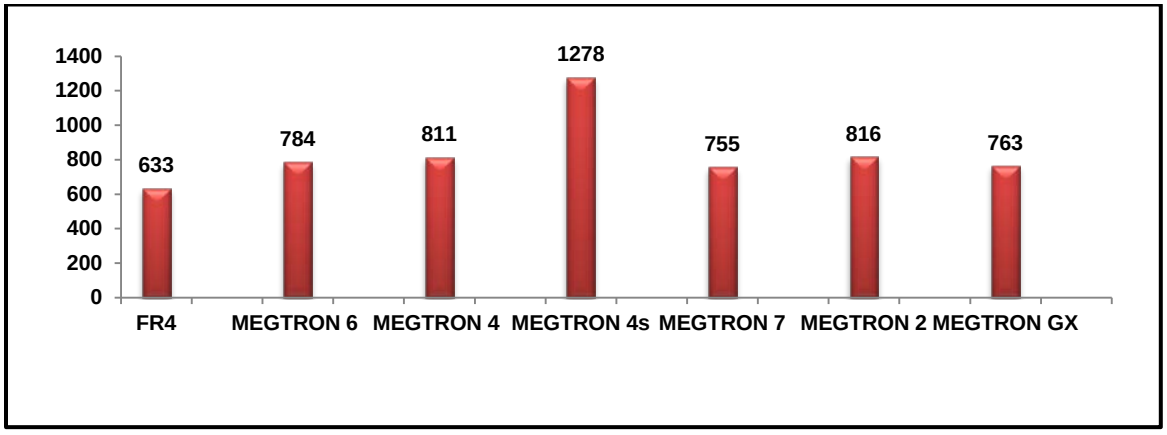

Figure 6.8: Plot for Life cycles to failure

In this work, material characterization of the boards was performed successfully using the DMA and TMA to obtain Young's Modulus and Coefficient of Thermal Expansion which were used for computational analysis. Results were analyzed for the obtained equivalents stresses, strains and directional deformation using Finite Element Analysis. Maximum stresses were observed on the corner solder ball towards the package side. It was concluded that the FR4 board show 14.48% more deformation as compared to the pf the Megtron 6 board. Megtron 6 boards are 24% more durable than FR4 board. The reliability of Megtron 6 and FR4 boards were compared and it was concluded that the Megtron 6 board is more durable and reliable than the FR4 board. Megtron 6 board has a decomposition temperature of about 410^{o}C and glass transition temperature of 210^{o}C which make is applicable to use for high temperature applications. As compared to FR4 boards, Megtron 6 has low dielectric constant, low dissipation factor, better impedance control and provides better performance. Cost of Megtron 6 is at least more than two times of FR4 board but the Megtron 6 boards are more reliable and durable. In future, a detailed layer by layer model can be constructed and analysis can be done to calculate change in plastic work and the effect of stresses and strain on the solder joint. Drop test can be performed using Megtron 6 boards. Power cycling can be performed similarly. Megtron 6 boards are used for large packages; similar study can be done for different large packages. Effect of moisture absorption on Megtron6 boards as compared to other boards can be studied.

APPENDIX

APDL SCRIPT USED FOR STRAIN ENERGY DENSITY

! Commands inserted into this file will be executed immediately after the

ANSYS /POST1 command.

! Active UNIT system in Workbench when this object was created: Metric (m, kg, N, s, V, A)

! NOTE: Any data that requires units (such as mass) is assumed to be in the consistent solver unit system.

! See Solving Units in the help system for more information.

!APDL SCRIPT TO CALCULATE PLASTIC WORK

/post1 allsel,all

!CALC AVG PLASTIC WORK FOR CYCLE1 set,5,last,1 !LOAD STEP

cmsel,s,botsolder,elem !ELEMENT FOR VOL AVERGAING

etable,vo1table,volu pretab,vo1table

etable,vse1table,nl,plwk !PLASTIC WORK

pretab,vse1table

smult,pw1table,vo1table,vse1table

ssum

*get,splwk,ssum,,item,pw1table

*get,svolu,ssum,,item,vo1table

pw1=splwk/svolu !AVERAGE PLASTIC WORK

!CALC AVG PLASTIC WORK FOR CYCLE2

set,10,last,1 !LOAD STEP

cmsel,s,botsolder,elem

etable,vo2table,volu pretab,vo2table

```
etable,vse2table,nl,plwk !PLASTIC WORK
pretab,vse2table
smult,pw2table,vo2table,vse2table
ssum
*get,splwk,ssum,,item,pw2table
*get,svolu,ssum,,item,vo2table
pw2=splwk/svolu !AVERAGE PLASTIC WORK
!CALC DELTA AVG PLASTIC WORK
pwa=pw2-pw1
!CALC AVG PLASTIC WORK FOR CYCLE3

set,15,last,1 !LOAD STEP
cmsel,s,botsolder,elem
etable,vo3table,volu
pretab,vo3table
etable,vse3table,nl,plwk !PLASTIC WORK
pretab,vse3table smult,pw3table,vo3table,vse3table
ssum
*get,splwk,ssum,,item,pw3table
*get,svolu,ssum,,item,vo3table
pw3=splwk/svolu !AVERAGE PLASTIC WORK
!CALC DELTA AVG PLASTIC WORK
pwb=pw3-pw2
```

REFERENCES

[1] Unique Rahangdale, “Mechanical Characterization of RCC and FR4 laminated PCB’s and assessment of their board level reliability”, IEEE Itherm 2017

[2] Advanced Power Management Unit, Texas Instruments, SLVSAJ2–August 2010

[3] John Coonrod, “Understanding When to use FR-4 Or High Frequency Laminates”, Onboard Technology September 2011

[4] Sanjay Mahesan Revathi, “Experimental and Computational analysis on the effect of PCB layer Copper thickness and prepreg layer stiffness on solder joint reliability” University of Texas at Arlington MS-thesis, May 2015.

[5] A. Schubert, R. Dudek, E. Auerswald, A. Gollbardt, B. Michel, H. Reichl, "Fatigue Life Models for SnAgCu and SnPb Solder Joints Evaluated by Experiments and Simulation," in ECTC, 2003

[6] Lau, John H., "Effects of Build-up Printed Circuit Board Thickness on the Solder Joint Reliability of a Wafer Level Chip Scale Package (WLCSP)".

[7] Sanny He, “New Halogen free & Low Loss Materials for High Frequency PCB Application”, IEEE 2008

[8] Tech Talk for Talkies,” Beyond FR-4: High Performance Materials for Advanced Designs”, May 2013

[9] Jeng-I Chen, “Characterization of Low Loss Materials for High Frequency PCB Application”, IEEE 2007

[10] M.S. Kaysar Rahim, “Board Level Temperature Cycling Study of Large Array Wafer Level Package”, Electronic Components and Technology Conference 2009

[11] Panasonic Material Properties, Panasonic

[12] Fahad Mirza, “Compact Modeling Methodology Development for Thermo-Mechanical Assessment in High-End Mobile Applications–Planar and 3d TSV Packages” University of Texas at Arlington PhD Thesis

[13] Unique Rahangdale, “Effect of PCB thickness on solder joint reliability of Quad Flat no-lead assembly under Power Cycling and Thermal Cycling”, IEEE 2017

[14] Sumanth Krishnamurthy, “Experimental and Computational Board Level Reliability Assessment of Thick Board QFN Assemblies Under Power Cycling”, University of Texas at Arlington, MS-thesis, May 2016

BIOGRAPHICAL INFORMATION

Mugdha Anish Chaudhari received her bachelor's in technology degree in Mechanical Engineering from Sardar Patel College of Engineering, Mumbai 2014. She pursued her master's in Mechanical Engineering in the University of Texas at Arlington in spring 2017. She was an active member of EMSPC reliability team and was also the Secretary of Surface Mount technology Association Student Chapter at the University of Texas at Arlington. Her research included experimental material characterization of printed circuit boards and thermo mechanical simulations of electronic packages. She was also a part of the SRC funded project where she worked with the industrial liaisons. After graduation she plans to pursue her career in the field of electronic packaging and semiconductors.